The Evaluation of Medium Voltage Motor's Current and Voltage Harmonics during Loading

Bora Alboyaci† and Nuran Yörükeren*

Abstract – This paper presents the results of investigating harmonic levels on medium voltage motors at loading conditions in air separation plant. The essential results of the measurements of the medium voltage motor harmonics are summarized in the values for the total harmonic distortion (THD). Motors loading case is used to assess the current and voltage harmonic distortions. Proper system analysis is important when adding a new motor starting and controlling the equipment. With the result of the paper it is possible to suggest the most appropriate starting and control method. Two medium voltage motors of air separation unit measurement results and simulations are summarized. Both current and voltage harmonic distortions are fitted by using a linear and exponential regression model. The prediction of THD values can be used for this kind of process for future planning by utilities.

Keywords: Medium Voltage Motor, Current and Voltage Harmonics, Motor Loading

1. Introduction

Motors have the undesirable effect of drawing several times their full load current while started. This large current will, by flowing trough system impedances, cause voltage sag that may dim lights, cause contactors to drop out, and interrupt sensitive equipment. The situation is made worse by an extremely poor starting displacement factor. The time required for the motor to accelerate to rated speed increases with the magnitude of the sag, and excessive sag may even prevent the motor from starting successfully [1].

There are several researches on motor starting and control methods for medium voltage motors [2-3]. This paper summarize common methods and provide application guidelines for proper choice selection considering the distribution system, driven equipment, speed-torque issues, starter method limitations and economics [3]. Interactions of reaccelerating motors dynamic simulations were chosen. The results of dynamic analysis are a plant where about 350 motors are assigned to automatic reaccelerating. The system involves massive restarting of motors on a power system that is already weakened by at least one contingency and without the benefit of off-loading motors. Therefore, all motors are restarted under full load condition [4]. Several authors are also interested in voltage sag that is caused from a motor which is energized. It has been seen how the deceleration and acceleration of motors influences duration and shape of voltage sags [5]. Taking motor behaviors into account will make it no longer possible to define sag simply by its duration and magnitude. The influence of motors on the shape of voltage sags is discussed in detail [5-6]. This paper presents the applications of regression models to predict the future growth trend of THD of 40 power transformers from field measurement data. The prediction values are important and can be used for transformer planning [7].

Many publications mention the influence of voltage sag on motor behaviors or voltage sags due to motor starting, but not the influence of motors approximately 'no load current spectra' to power quality. In chemical process all big air separation unit compressors are feeding from medium voltage and these motors reach their nominal load about 7-8 hours. If there are more than one motor supplied from a bus and no countermeasures are taken, existing harmonic distortions can reach dangerous limits.

2. System Description

2.1 Process Description

Air separation plants produce nitrogen, oxygen and argon using air and electrical power as raw materials. The basic process for large-scale air separation process has remained unchanged for decades [8-9]. An air separation plant consists mainly of the following five steps in Fig. 1.:

- Filtering and compressing air, see Filter and motor M1,

† Corresponding Author: Dept. of Electrical Engineering, The University of Kocaeli, Turkey. (alboyaci@kou.edu.tr)
* Dept. of Electrical Engineering, The University of Kocaeli, Turkey. (nurcan@kou.edu.tr)
Received 25 August, 2006 ; Accepted 10 January, 2007

- Removing contaminants, including water vapor and carbon dioxide (which would freeze during the process),
- Cooling the air to very low temperature through heat exchange and refrigeration processes,
- Distilling the partially-condensed air (at about -300°F / -185°C) to produce desired products,
- Warming gaseous products and waste streams by heat exchange with incoming air.

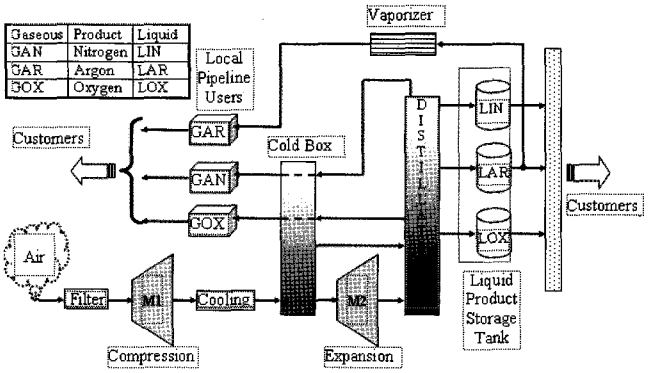

Fig. 1. Gas production flow outline.

All air separation processes start with compression of air. Electric power is used to drive most of the compression equipment. Additional compression equipment may be used to raise product gas pressures to the required distribution pressure. More compressors are used to produce additional refrigeration when liquids are produced. Purchase of electricity is the largest operating cost incurred in air separation plants. When the two motors M1 and M2 are loaded to their nominal load, liquid and gas phase production starts. Plants daily liquid phase production capacity is approximately 140 Ton/day. It consists of 120 T/day LOX, 15 T/day LIN and 5 T/day LAR.

2.2 Electrical Description

Air separation plant which is examined for this study installed power is 35 MVA. The plant is feeding from 154/34.5 kV substation. There are three transformer ratings; 30 MVA and 34.5/6.3 kV, 2500 kVA and 34.5/0.4 kV, and 1000 kVA 34.5/0.4 kV. There are two medium voltage motors which names are M1 and M2. A 30 MVA power transformer supply M1 and M2 motor's electrical consumption. Also medium voltage motors are started with direct online start and unloaded. M1 and M2 motor's reactive power compensation is done locally. Compensation groups are connected star and withstand 7.2 kV.

After filtering, the air is compressed by motor M1. The compressed air is afterwards cooled down to close-to-ambient temperature by passing through water-cooled or air-cooled heat exchangers. The cooling period is approximately 5 hours long and the cooling temperature is about -185°C. During the cooling period motor M2 is switched off. The cooling is accomplished with cold product and waste gas streams exiting the separation process.

When proper conditions are met, motor M2 is switch on. After that motor M2 is loaded step by step and reaches nominal load after about 3-4 hours. Distillation columns separate the air into the desired products. Oxygen plants will have both high and low pressure columns where impure oxygen from the high-pressure column receives further purification in the low-pressure column. Nitrogen plants may have only one column, although some also have two columns. Because the boiling points for oxygen and argon are similar, plants producing very high purity oxygen require more distillation stages and remove argon from near the mid-point of the low pressure column where its concentration is highest. The parameters of medium voltage motors are given in Table 1.

Table 1. Induction motor parameters

MOTOR	M1	M2
R_s (ohm)	0,0423	0,0759
X_s (ohm)	1,4713	1,6094
X_m (ohm)	69,43	75,35
R_r (ohm)	0,0423	0,0526
X_r (ohm)	1,1323	1,1668
H (kgm^2)	45	50
S (kVA)	1828	2851
V (kV)	6,3	6,3

Along with the aforementioned basic information, which is required for a voltage drop type of motor starting analysis, several other items are also required for the detailed speed-torque and accelerating analysis. These include speed-torque characteristic of both the motor and the load.

3. Simulated and Measured Industrial System Values

3.1 Site Survey

Fig. 2 shows a picture of measurement at the secondary site of a 30 MVA transformer. Three power analyzers are used to measure system parameters. One of the power analyzers is Fluke 199-C scope meter and the others are Circutor AR5 network power analyzers. The maximum

magnitude and time of the motors' inrush currents' are measured with the scope meter Fluke 199-C (200 MHz). To sampling rate is set to 1250 Hz (or 24 samples for one 50 Hz period) which satisfies the Nyquist criterion. After the motors have been switched on to reach nominal load conditions, the Circutor AR5 network analyzers measure currents, voltages, total harmonic distortions and individual harmonic distortions. Circutor AR5 starts a new analysis every 5 seconds. Periodic variations in current and voltage magnitudes and harmonic distortion levels can then be studied more precisely.

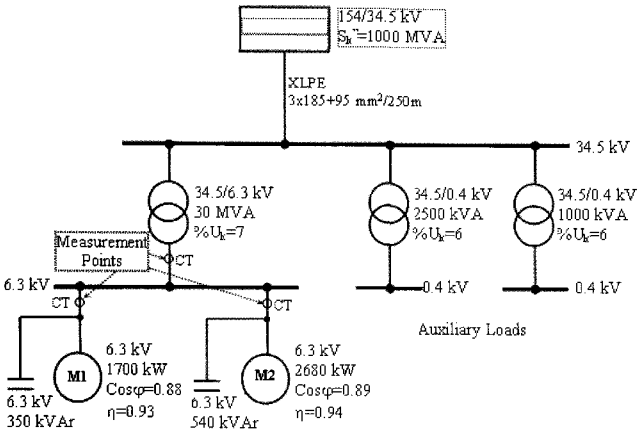

Fig. 2. Single Line Diagram of Electrical Separation Unit

In Fig. 3 it is shown how motor M1 is started at 09:07, electrical data are stored simultaneously. Motor M1's inrush current peak is determined to 950A. It is approximately 5.1 times the nominal current of the motor. After motor M1's initial inrush conditions have passed, the "no load" current is measured to 66A. M1 motor's current is reached 102,5 A at 17:20. These values are showed at Fig. 3.

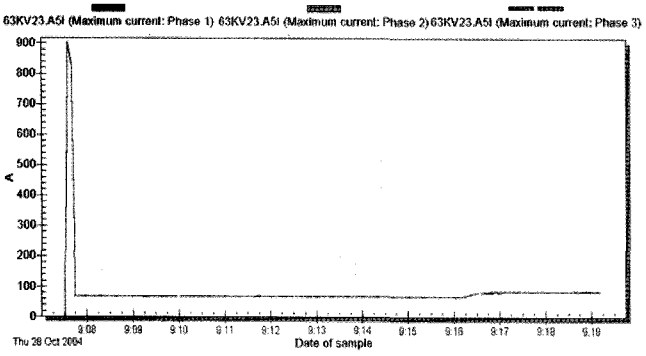

Fig. 3. Motor M1's current deviations

After appropriate system conditions, motor M2 is switched on manually. Motor M2's inrush current is 1300A as shown in Fig. 4. It is approximately 4.7 times greater than the nominal current which is 267A. After motor M2's inrush conditions have passed, no load current is 74A. Motor M2 is loaded step by step. These values are shown in Fig. 4.

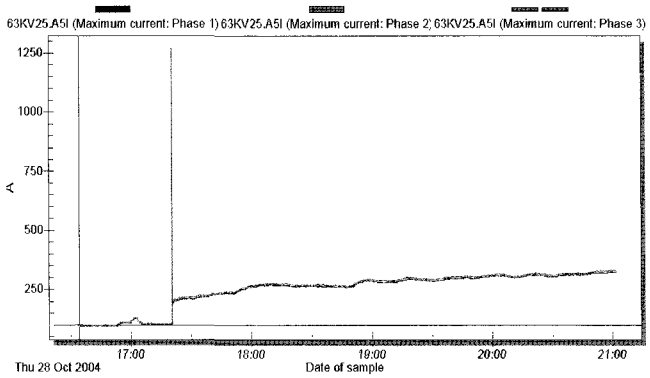

Fig. 4. Motor M2's current deviations

In this way motor inrush currents peak and period value is not determined by exactly. For this reason these currents are measured at the same time with Fluke 199C energy analyzer. Measured values are given in Fig. 5a and 5b. Motor M1's and motor M2's inrush conditions are completed 5.7s and 6.4s under no load, respectively. Maximum starting currents and starting periods of both motors are shown in the figures.

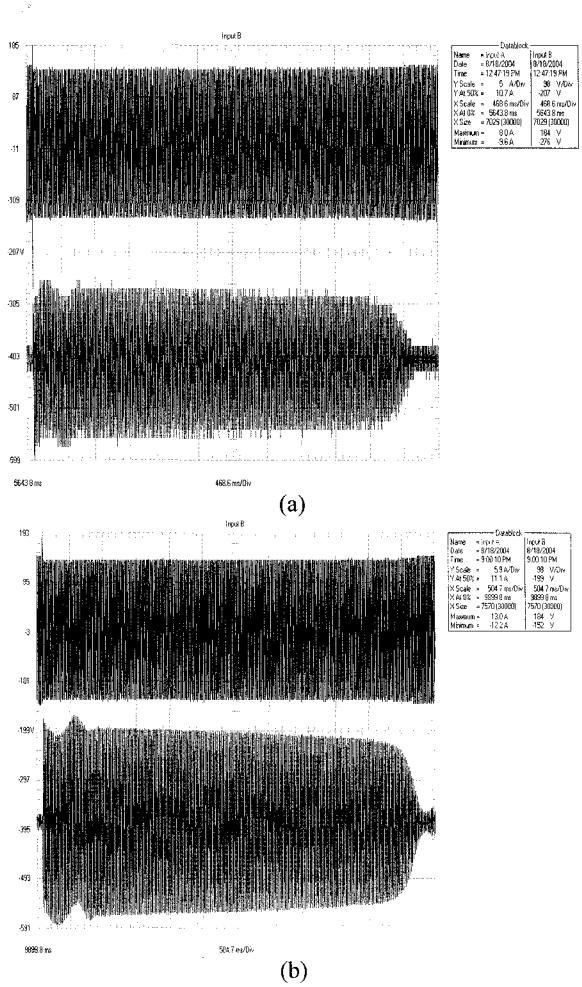

(a)

(b)

Fig. 5. Current and voltage variations of motors at starting a) Motor M1 b) Motor M2

All current and voltage signals contain 30.000 samples each. The starting of induction motors M1 and M2 leads to voltage drop. The rms value of motor's terminal voltage is calculated in order to better understand the voltage drop. The rms value is calculated within every cycle. This is done by using the following equation:

$$V_{RMS}(kN) = \sqrt{\frac{1}{N}\sum_{i=(k-1)N+1}^{i=kN} v_i^2} \quad (1)$$

Where N is the number of samples per cycle, v_i is the sample voltage (the instantaneous value) in the time domain [10]. The algorithm described in equation (1) has been applied to the voltage drop shown in Fig. 6. In Fig. 6 the rms voltage has been calculated over a window with a width of one cycle, which was 24 samples for the recording used.

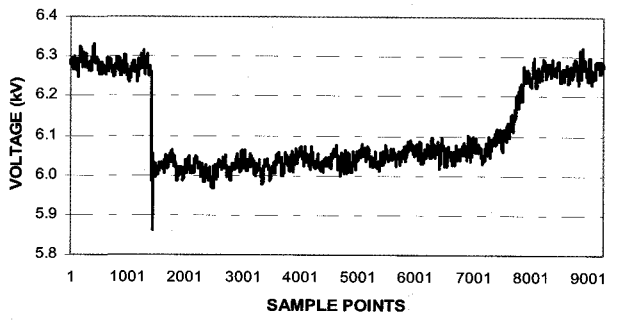

(a)

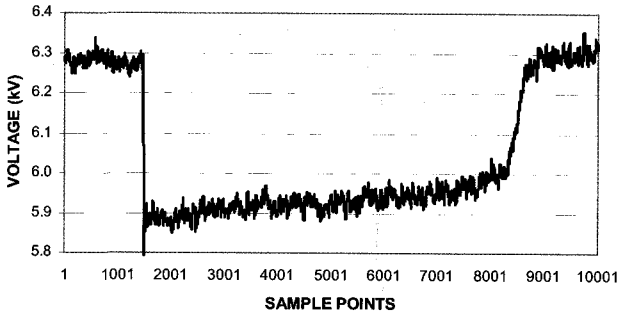

(b)

Fig. 6. a) Motor M1 voltage drop, b) Motor M2 voltage drop

3.1 Simulation Study

To check and prove the correctness of Fig. 6 we have done simulations with power system simulation software of the investigated power system. The required calculations are complicated and in order to analyze the motor starting a general transient analysis computer program have been used. Parameter values for standard induction motor equivalent circuit, number of motor poles and rated rpm, inertia constant values for the motor and the motor load, torque versus speed characteristic for the motor load data are required for the simulations and can be found in section 2.2.

The used simulation software is Simpow [11]. In contradiction to other analyze programs; Simpow is examining motor parameters rotor resistance change depending in the slip [11]. The software has two modes of time-domain simulations. The instantaneous value mode, the Masta-mode, simulates instantaneous values of voltages and currents of the network and other primary components of the power system, while the fundamental frequency mode, the Transta-mode, simulates power-frequency components only, expressed as phasors. In this study, the Transta-mode is used.

For this reason, slip values bound to the rotor resistance are calculated from the motor characteristics. In Fig. 7 the analyses done with the obtained motor and load characteristics and system parameters are shown. In Fig. 6, the same results with the measurement values are shown. Voltage drop values at Fig. 6 and simulation results in Fig. 7 are similar; however, the differences can come from incorrect setting of the parameters of the power system. The general trend of the sag is however similar in the measurements as well as in the simulations.

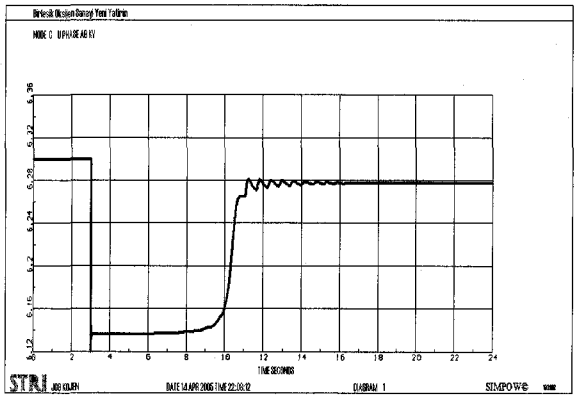

(a)

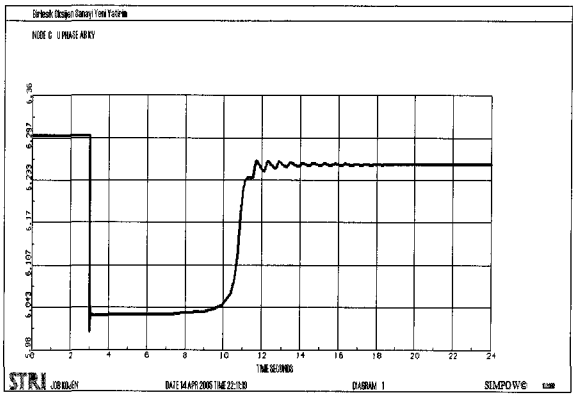

(b)

Fig. 7. Simulated voltage drops of motors a) M1, b) M2.

4. Current and Voltage Deviation during the Motor Loading

4.1. Linear Regression

The motor' loading currents versus time is shown in Fig.3 and 4. The loading currents versus THD_I and THD_V are represented in Fig. 8 for motor M2. From Fig. 8 it is obvious that THD_I and THD_V follow the variation of the load current. In order to obtain the information after the load grows, regression model analyses have been adopted. It can predict the dependent variable, y_i, as a linear function on the independent variable, x_i. In order to predict THD_I and THD_V levels from motor loading current, regression model is adopted. In this work, background harmonic voltage levels have been neglected.

The task of estimation is to determine regression coefficients β_0 and β_1, estimates of the unknown parameters β_0 and β_1 respectively. The estimated equation will have the form:

$$\hat{y} = \beta_0 + \beta_1 . x \tag{2}$$

where x is the load current and $\hat{y}$ is the estimate of THD_I (THD_V).

The basic technique for determining the coefficients β_0 and β_1 is Ordinary Least Squares (OLS), values for β_0 and β_1 are chosen so as to sum of the squared residuals (SSR).

$$\begin{aligned} \beta_0 &= \bar{y} - \beta_1 . \bar{x} \\ \beta_1 &= \frac{\sum (x_i - \bar{x})(y_i - \bar{y})}{\sum (x_i - \bar{x})^2} \end{aligned} \tag{3}$$

where x_i is the load current at the ith observation; y_i is the THD_V or THD_I at the ith observation; x is the mean value of load current; y is the mean value of THD_V or THD_I.

4.2. Exponential Regression

For curve lines, the exponential regression model is more precise than the linear regression. At first, the following transformation model is used;

$$y' = \ln(y) \tag{4}$$

Then the linear regression model as that in Equation (2) is obtained:

$$\hat{y}' = b_0' + b_1(x) \tag{5}$$

And the exponential form is,

$$\hat{y} = \exp(\hat{y}') = b_0 \exp(b_1 . x) \tag{6}$$

Where $b_0 = \ln b_0'$

In order to identify the goodness of fitting a regression model to the measurement data, the coefficient of determination R^2 is used as;

$$R^2 = \frac{\sum (\hat{y}_i - \bar{y})}{\sum (y_i - \bar{y})^2} \tag{7}$$

The value of R^2 is between 0 and 1. The closer the value of R^2 is to 1, the stronger the relationship is to predict a correct value of y. In order to get harmonic information of a power system, field measurement is for a utility the best way. Motor feeding bus' harmonic voltage distortions follow with harmonic current distortions, that is, motors are harmonic sources. Regression models can provide a good tool for predicting loading trend of harmonic distortions.

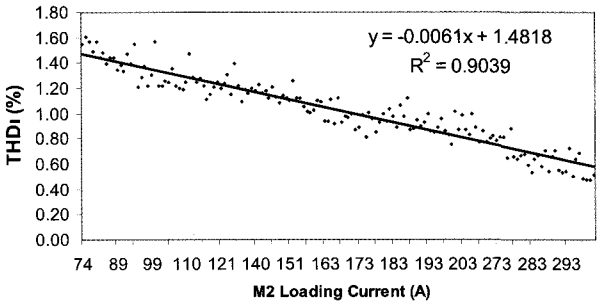

(a) Linear regression

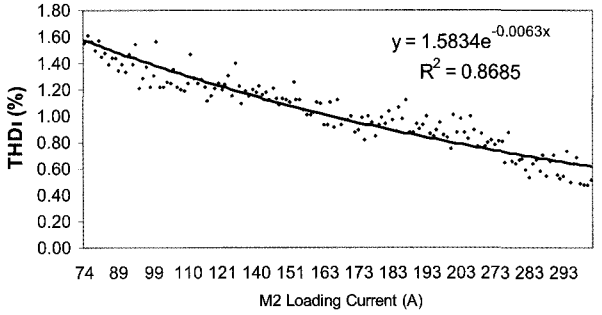

(b) Exponential regression

Fig. 8. The regression models of THD_I versus load current of motor M2

With measurement data in Fig.8, the regression models of THD_I versus load current for the motor M2 is represented in Fig 8a-8b, respectively.

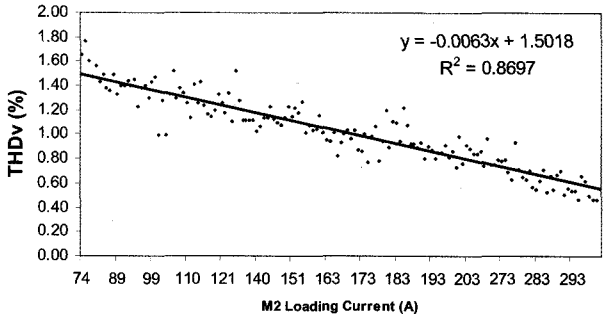

(a) Linear regression

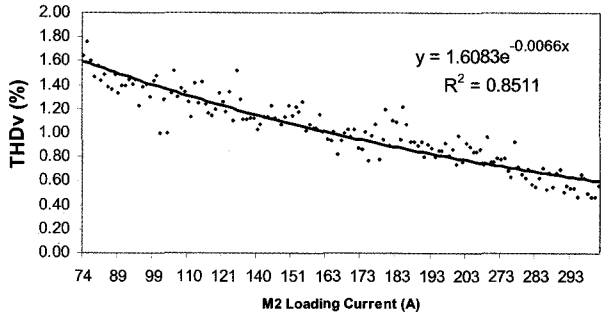

(b) Exponential regression

Fig. 9. The regression models of THD_V versus load current of motor M2

With measurement data in Fig.9, the regression models of THD_V versus load current for the motor M2 is represented in Fig 9a-9b, respectively.

The other results are shown in Table 2. Linear regression R^2 values are for both THD_I and THD_V better than exponential regression values.

Table 2. Linear and exponential regression models of THD_I and THD_V versus load current of medium voltage motors

Motor	THD	Regression Type	Equation	R^2
M1	THD_I	Linear	$-0{,}0061.I_L+1{,}4818$	0,9039
	THD_I	Exponential	$1{,}5834e^{-0{,}0063.I_L}$	0.8685
	THD_V	Linear	$-0{,}0063.I_L+1{,}5018$	0,8697
	THD_V	Exponential	$1{,}6083e^{-0{,}0066.I_L}$	0.8511
M2	THD_I	Linear	$-0{,}0051.I_L+1{,}5878$	0,9539
	THD_I	Exponential	$1{,}5134e^{-0{,}0060.I_L}$	0.8941
	THD_V	Linear	$-0{,}0066.I_L+1{,}3018$	0,8277
	THD_V	Exponential	$1{,}5277e^{-0{,}0049.I_L}$	0.8021

Fig. 10 shows addition of motor M1 and motor M2 loading current versus THD_I (%). Motor M1 reaches nominal current at 112 A during the 5 hours. Motor THD_I (%) decreases from 1,6% to 0.7% throughout the loading. Motors THD_V (%) deviations are the same as THD_I (%). It is represented in Fig. 11. When first motor reaches nominal current and to meet system conditions motor M2 approximately started at 120 A. Feeder current reaches from 120 A to 300 A approximately 3 hours.

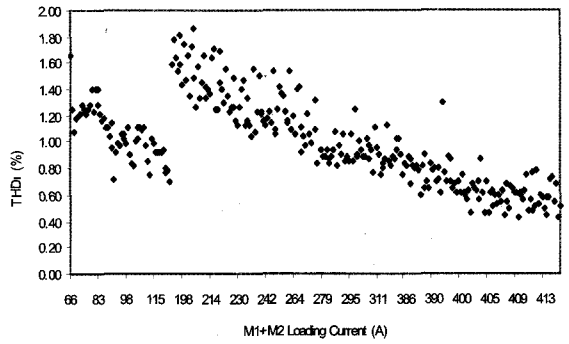

Fig. 10. THD_I (%) versus load current M1+M2

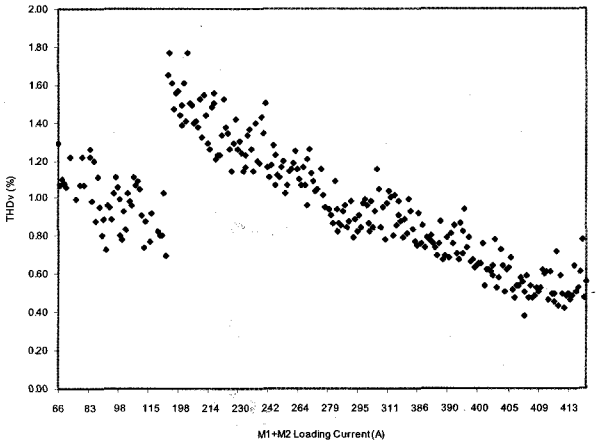

Fig. 11. THD_V(%) versus load current motor M1+M2 motor

5. Conclusion

In many parts of the world, the actual voltage distortion levels are maintained within the planning level by imposing appropriate emission limits to the harmonic line current limits. To determine appropriate equipment emission limits, both measurement campaigns and simulations are required to study the harmonic propagation in a network. This paper presents the applications of regression models from measurement data predict for total harmonic distortions on coordination loading. The method is tested on an existing air separation plant by using both simulations and field measurements. Results are promising. The method of predicting values are can be used by the utility for future planning.

Acknowledgements

This work was supported by the The University of KOCAELI and ABB Turkey.

References

[1] R.C. Dugan, M.F. McGranaghan, S. Santoso, H.W. Beaty, "Electrical Power Systems Quality", *McGraw Hill*, 2002.

[2] J.A. Kay, R.H. Paes, G. Seggewiss, R.G. Ellis "Methods for the Control of Large Medium Voltage Motors: Application Considerations and Guidelines", *IEEE Transactions on Industry Applications*, pp. 1688-1696, Vol.36, No.6, 2000.

[3] G.S. Greval, S. Poscai, M.M. Hakim, "Transient Motor Reacceleration Study in an Integrated Petrochemical Facility", *IEEE Transactions on Industry Applications*, pp. 968-977, Vol.35, No.4, 1999.

[4] Math H.J. Bollen "The Influence of Motor Reacceleration on Voltage Sags", *IEEE Transactions on Industry Applications*, pp. 667-673, Vol.31, No.4, 1995.

[5] J.C. Das, "The Effects of Momentary Voltage Dips on the Operation of Induction and Synchronous Motors", *IEEE Transactions on Industry Applications*, pp. 711-718, Vol.26, 1990.

[6] J.J. Wu, C.H. Hu, C.C. Yin, C.C. Chiu, "Application of Regression Models To Predict Harmonic Voltage and Current Growth Trend From Measurement Data at Secondary Substations", *IEEE Transactions on Power Delivery*, pp. 793-799, Vol.13, No.3, 1998.

[7] Universal Industrial Gases Inc., www.uigi.com/cryodist.html, 2005.

[8] British Oxygen Company Inc., www.boc.com, 2005.

[9] Math H.J. Bollen "Understanding Power Quality Problems", IEEE *Press Series on Power Engineering*, 1999.

[10] SIMPOW Power System Simulation & Analysis Software, *Release 10.8, Copyright(c) STRI AB*, 2004.

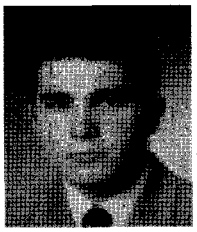

Bora Alboyaci

He received the B.Sc. degree in electrical engineering in 1995 from the Technical University of Yildiz. He received the M.Sc. and Ph.D. degreesin electrical engineering in 1998 and 2001 respectively from The University of Kocaeli. From 1995 to 1996, he worked for TEMAS Consulting Engineering, and his last position was a Consultant Engineer. Since 2001, he has been working as an Assoc. Prof. Dr. at The University of Kocaeli. He is leading two projects concerning power quality of distribution systems and distribution transformer loading evaluations.

Nuran Yörükeren

She received the B.Sc. degree in electrical engineering in 1988 from the The University of Yildiz. She received the M.Sc. and Ph.D. degrees in electrical engineering from the University of Kocaeli. She has been working as a Assoc. Professor at The University of Kocaeli. She has been working in an administrative affair. Her areas of interests include power system planning, energy transmission and distribution, optimization of power plants, and power system analysis.